SURFACE SCIENCE 13 (1969) 151–171 © North-Holland Publishing Co., Amsterdam

FORWARD CURRENT-VOLTAGE CHARACTERISTICS OF SCHOTTKY BARRIERS ON n-TYPE SILICON

A. N. SAXENA

Research and Development Laboratories, Sprague Electric Company, North Adams, Massachusetts 01267, U.S.A.

Received 10 July 1968; revised manuscript received 7 August 1968

An analysis of the forward I–V data of the Schottky barriers formed by Au, Ni and Cr on n-type Si, and of two commercially available Schottky barrier diodes (Fairchild's FH-1100 and Hewlett–Packard's HP-2900) is presented. When the fringing high electric fields at the edge of the diodes are eliminated by using guard rings or mesa structures, their I–V behavior is given by $I = I_s\,[\exp\{qV/k(T+T_0)\} - 1]$, where T_0 is a constant. When the fringing high electric fields are not eliminated, thermionic-field (T–F) emission is observed, which increases T_0 at low temperatures. Activation energy plots of $\ln(I_s/T^2)$ versus $1/T$ are not linear for guard ring or non-guard ring diodes implying that the barrier height, ϕ_{MS}, varies with temperature. Plots of $\ln(I_s/T^2)$ versus $1/(T+T_0)$ are found to be linear for either kind of diode, which give effective barrier heights, ϕ_{MS0}, independent of temperature. For non-guard ring diodes, T_0 varied with temperature and it was calculated at each temperature; for guard ring diodes, T_0 was approximately a constant with respect to temperature. Therefore, the saturation current I_s is given by $I_s = A^*T^2 \exp\{-\phi_{MS0}/k(T+T_0)\}$. A model employing temperature dependence of the barrier height, ϕ_{MS}, in the simple Schottky theory is given which explains, qualitatively, T_0 and ϕ_{MS0}.

1. Introduction

A rectifying metal–semiconductor contact is generally known as a Schottky barrier[1]). The barrier height, ϕ_{MS}, governing the electrical behavior of such a junction is predicted by two models in the extreme cases defined below.

1) *Surface state model.* The barrier height ϕ_{MS} on a given semiconductor is independent of the metal used[2,3]). This is considered to be valid when the surface-state density on the semiconductor surface is large (> about 10^{14} cm^{-2}). That such a condition exists on cleaved semiconductor surfaces is implied from the results of Mead and Spitzer[3]). For n-type semiconductors it was found that,

$$\phi_{MSn} \simeq \tfrac{2}{3}E_G\,, \tag{1}$$

where E_G is the energy gap of the semiconductor. For p-type semiconductors, it was found that,

$$\phi_{MSp} \simeq \tfrac{1}{3}E_G\,. \tag{2}$$

As is evident from eqs. (1) and (2), the temperature dependence of the barrier height will follow that of the band gap of the semiconductor. This was observed by Crowell et al.[4]) for the case of Au on n-type Si Schottky barrier.

2) *Work function difference model.* The barrier height ϕ_{MS} is governed by the difference in the work function[5]) of the metal ϕ_M and that of the semiconductor $\phi_s = \chi + \phi_F$, where χ is the electron affinity (defined here to be the energy required to remove an electron from the bottom of the conduction band to the vacuum level), and ϕ_F is energy difference between the Fermi level and the bottom of the conduction band. The energy band diagram is shown in fig. 1 for an n-type semiconductor for which the condition to get a rectifying contact is $\phi_M > \phi_s$. The barrier height ϕ_{MS} is given by,

$$\phi_{MSn} = \phi_M - \chi . \tag{3}$$

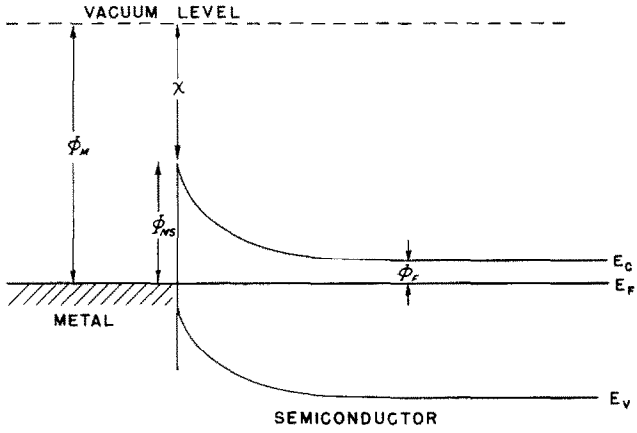

Fig. 1. Energy band diagram for Schottky barrier formation on n-type semiconductor.

Henceforth, the letter n in the subscript for ϕ_{MS} will be deleted because we shall discuss Schottky barriers on n-type Si only. It is clear from eq. (3) that if the Schottky barrier is formed under conditions for which the work function difference model holds, then the barrier height will vary with the work function of the metal ϕ_M assuming that χ is unaffected by different metals. Further, the temperature dependence of ϕ_{MS} will follow that of ϕ_M if the temperature dependence of χ is negligible as compared with that of ϕ_M. The above two features distinguish this model from the surface-state model.

The I–V behavior of a Schottky barrier is given theoretically by[1,5])

$$I = A^* T^2 \, e^{-\phi_{MS}/kT} \left[e^{qV/kT} - 1 \right], \tag{4}$$

where A^* is the effective Richardson constant and the rest of the symbols

have their usual meanings. At a given temperature T, eq. (4) predicts that for $V \gtrsim 3\,kT/q$, ln I versus V will be linear with unity slope. The intercept at $V=0$ of such a straight line will give a saturation current I_s defined by,

$$I_s = A^* T^2 \, e^{-\phi_{MS}/kT}. \tag{5}$$

When such I–V plots are made at various temperatures and I_s determined, and when I_s/T^2 is plotted versus $1/T$ (known generally as the activation energy plot), then another straight line should be obtained whose slope should give the value of ϕ_{MS}. *However, the above activation energy plot will be a straight line only when ϕ_{MS} is a constant with respect to temperature or has a linear temperature dependence.*

Atalla et al.[6]) found that their experimental I–V data on Schottky barriers fitted the following equation:

$$I = I_s(e^{qV/nkT} - 1). \tag{6}$$

In eq. (6), n is a constant >1, usually between 1 and 1.1. Atalla et al. used the constant n in the exponent in analogy with the recombination-generation currents in the I–V behavior of p–n junctions. Sze et al.[7]) showed that such a value of n can approximately be accounted for when the image forces are taken into account.

Padovani and Sumner[8]) first reported that their I–V data of a Au–GaAs Schottky barrier fitted the following equation:

$$I = I_s[e^{qV/k(T+T_0)} - 1]. \tag{7}$$

In eq. (7), T_0 referred to as the excess temperature is a constant >0. For Au–GaAs, it was found to be 50 ± 5°K. At a given temperature, n can be related to T_0 as,

$$n = 1 + T_0/T, \tag{8}$$

however, if T_0 is a constant, then n will no longer be a constant as the temperature is varied. When thermionic-field emission and field emission are assumed to be the dominant mechanisms in the I–V behavior of the Schottky barrier diode, then eq. (4) is further modified as explained below.

The significance of the deviations referred to above from the Schottky equation, eq. (4), is easily understood when it is written as,

$$I = I_s(e^{V/V_0} - 1). \tag{9}$$

For the voltage range of interest where $V/V_0 \gtrsim 3$, eq. (9) may be written as,

$$I = I_s \, e^{V/V_0}. \tag{10}$$

When ln I is plotted versus V, a straight line is obtained whose slope gives V_0 and its intercept at zero volt gives I_s. In a practical case when a diode of

small geometry is studied, ln I versus V deviates from the straight line due to series resistance. For an accurate determination of V_0 and I_s in such a case, the procedure of Saxena and Varady[9]) is used. From the I–V plots at various temperatures (the range studied here was $-100\,^{\circ}C$ to $+150\,^{\circ}C$), V_0 is found. When V_0 is plotted versus kT/q, the following five cases may be observed as shown in fig. 2.

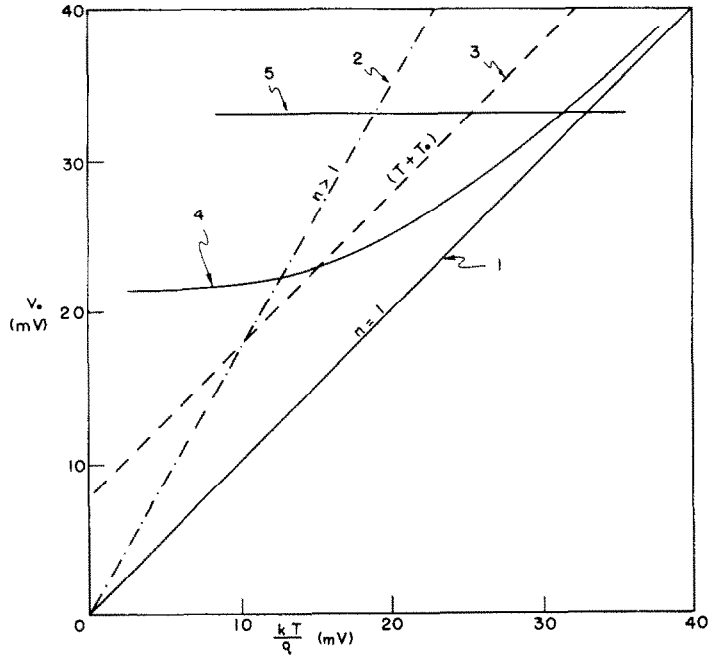

Fig. 2. Plot of V_0 (slope of ln I_F versus V_F) versus kT/q. Various lines refer to agreement with (line labelled as 1) or deviations from (lines labelled 2–5) the Schottky theory. See discussion in section 1.

1) If the diode obeys ideal Schottky theory, eq. (4) the V_0 data will lie on the straight line labelled 1 in fig. 2, which has unity slope, i.e.,

$$V_0 = kT/q\,. \tag{11}$$

2) If the diode obeys eq. (6), then the V_0 data will lie on the straight line labelled 2 in fig. 2 whose slope is >1, i.e.,

$$V_0 = nkT/q\,. \tag{12}$$

where n is a constant >1 and it is independent of temperature.

3) If the diode obeys eq. (7), then the V_0 data will lie on the straight line

labelled 3 in fig. 2, which is parallel to the unity slope line labelled as 1. In this case,

$$V_0 = k(T + T_0)/q\,, \tag{13}$$

where T_0 is a constant >0 and it is independent of temperature.

4) If the diode obeys thermionic-field emission (T–F) theory of Padovani and Stratton[10]), then the V_0 data will lie on a curve like the one labelled as 4 in fig. 2. In this case,

$$V_0 = V_{00} \coth(V_{00}/kT)\,, \tag{14}$$

where

$$V_{00} = \tfrac{1}{2}\hbar\,[N/m^*\varepsilon_0\varepsilon]^{\frac{1}{2}}\,. \tag{15}$$

In eq. (15), N is the impurity concentration in the semiconductor, ε is the dielectric constant of the semiconductor, m^* is the effective mass of the electrons and the rest of the symbols have their usual meanings. If eq. (7) is used to fit the I–V characteristic of a diode in which thermionic-field emission described above is present, then in this case T_0 is not constant with respect to temperature. It increases at lower temperatures.

5) If field emission dominates, then the V_0 data will lie on a straight line labelled as 5 in fig. 2. In this case, V_0 is independent of temperature and,

$$V_0 = V_{00}\,, \tag{16}$$

where V_{00} is defined by eq. (15).

The diodes studied in this investigation were the following (fabricated at the Sprague Electric Company):

1) Cr–Si, Au–Si and Ni–Si (all without guard ring),

2) Cr–Si with a guard ring.

Two commercially available diodes were also studied FH-1100 manufactured by Fairchild, and HP-2900 manufactured by Hewlett-Packard.

Section 2 describes the experimental procedure; the I–V data and their analyses are given in section 3. The I–V data of Au–Si, Ni–Si and Cr–Si diodes obeyed eq. (7) fairly well except for a deviation at the lower temperature of the range studied. Since these diodes did not have guard rings, high electric fields are present at the edges of the diodes causing some T–F emission to occur. Such deviation could not be explained by the T–F emission theory[10]). Similar behavior was observed for Fairchild's FH-1100.

For the Cr–Si diode with the guard ring structure, the deviation referred to above at low temperatures was not observed, and the I–V data obeyed eq. (7) quite well. The guard ring eliminated the high electric fields at the edge of the diode. It is inferred that these high electric fields are responsible for the deviation at low temperatures and contribute to T–F emission. Similar behavior was observed for Hewlett–Packard's HP-2900. It was found

that this diode had a built-in Au guard ring and a mesa structure which eliminate the high electric fields at the edges.

Section 4 describes the activation energy analysis to determine the barrier heights ϕ_{MS}. It was found that the plot of $\ln(I_s/T^2)$ versus $1/\mathbf{T}$ could not be fitted with a straight line; however, a linear fit could be obtained for $\ln(I_s/T^2)$ versus $1/(T+T_0)$ plot. This result further reinforces the validity of eq. (7) to describe the I–V behavior of Schottky barriers. The mechanism which could be considered to be responsible for the excess temperature T_0 is discussed in section 5.

2. Experimental procedure

The Schottky barrier diodes fabricated in this laboratory used an epitaxial n/n^{++}, (111) Si substrate. The resistivity of the epitaxial layer was in the range 0.2–0.4 Ω-cm and its thickness was 2–3 μm. The Si wafers were oxidized to grow a passivating SiO_2 layer. Standard photolithographic techniques were used to etch circular areas (of diameter 1 mil for Au and Ni diodes and 0.8 mil for Cr diodes) through the SiO_2 layer. After removing the oxide from the Si surface in the active area by chemical etching, Au, Ni or Cr was evaporated to fabricate the corresponding Schottky barrier diode. Appropriate precautions were taken to insure adherence of these metal films on the SiO_2 surface. Again, using standard photolithographic techniques, the metallization pattern was etched which allowed thermo-compression bonding to be done on top of the oxide to make contact to the Schottky barrier. This way, the Schottky barrier on Si was undisturbed by bonding. Fig. 3 shows a cross section of the device structure (not drawn to scale).

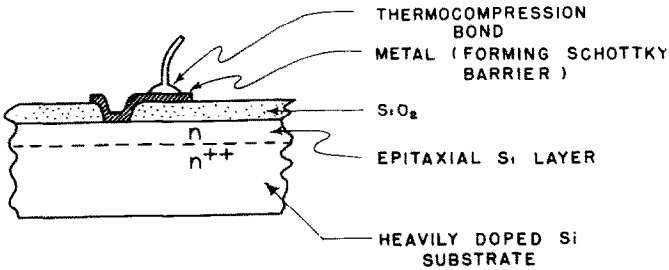

Fig. 3. Cross section of the Schottky barrier diodes fabricated at the Sprague Electric Company.

Fig. 4 shows a cross section of the guard ring diode. The active area of the Cr–Si Schottky barrier is surrounded by a guard ring of Au–Si barrier. The barrier height of the latter is greater than that of the former, i.e., $\phi_{Au-Si} > \phi_{Cr-Si}$. This has the effect of eliminating the high fields from the

edge of the Cr–Si diode. The I–V characteristics of such a structure are governed by the Cr–Si barrier because of the lower barrier height ϕ_{Cr-Si}.

The I–V characteristics of the above diodes were plotted at various temperatures (-100 °C to $+150$ °C) using a Delta Design Oven, Model No. MK2800. The accuracy of the temperature setting was within 1 °C.

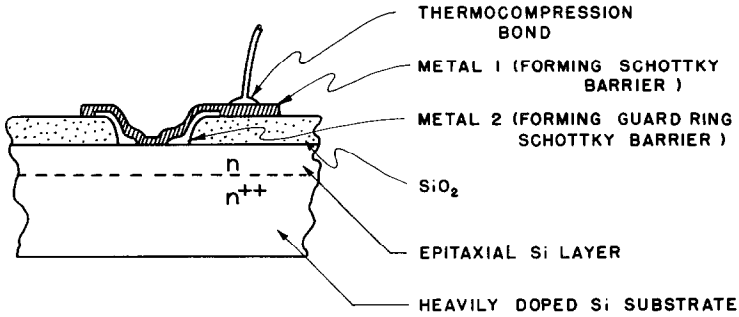

Fig. 4. Cross section of the Schottky barrier diodes with a guard ring fabricated at the Sprague Electric Company.

3. V_0 data from I–V plots

For voltages $V \gtrsim 3\,kT/q$, ln I versus V will be a straight line as predicted by eq. (10). The change in the voltage, ΔV, for a decade change in I is related to V_0 as,

$$V_0 = \Delta V/2.3026\,. \tag{17}$$

The values of V_0 were determined by fitting the ln I versus V plots with a straight line at various temperatures. At higher temperatures where the data deviated from a straight line, the procedure of Saxena and Varady[9]) was used for an accurate determination of V_0.

Figs. 5, 6, 7 and 8 show the V_0 versus kT/q data for Au–Si, Ni–Si, Cr–Si and FH-1100 diodes, respectively. In comparing the behavior of the data with fig. 2, it is observed that the data could be fitted with a straight line parallel to the unity slope line similar to the straight line labelled as 3 in fig. 2. The V_0 data at low temperatures deviated from the straight line. (See discussion in section 4.) It must be borne in mind that these diodes do not have a guard ring structure, therefore, high electric fields at the edges of the diode are present.

Fig. 9 shows the V_0 versus kT/q data for the Cr–Si diode with the Au–Si guard ring which has the effect of eliminating the high electric fields from the edge of the Cr–Si diode. It is observed that the data can be fitted quite well with a straight line parallel to the unity slope line, similar to the unity

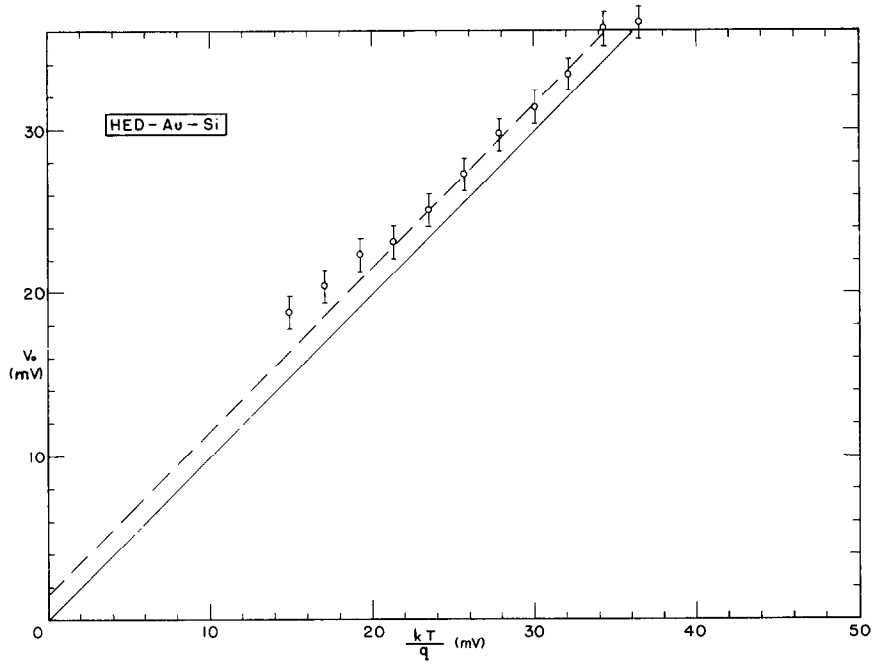

Fig. 5. Plot of V_0 versus kT/q for Au–Si Schottky barrier diode. Dashed line is drawn parallel to the unity slope (solid) line to illustrate deviation from eqs. (4) and (7).

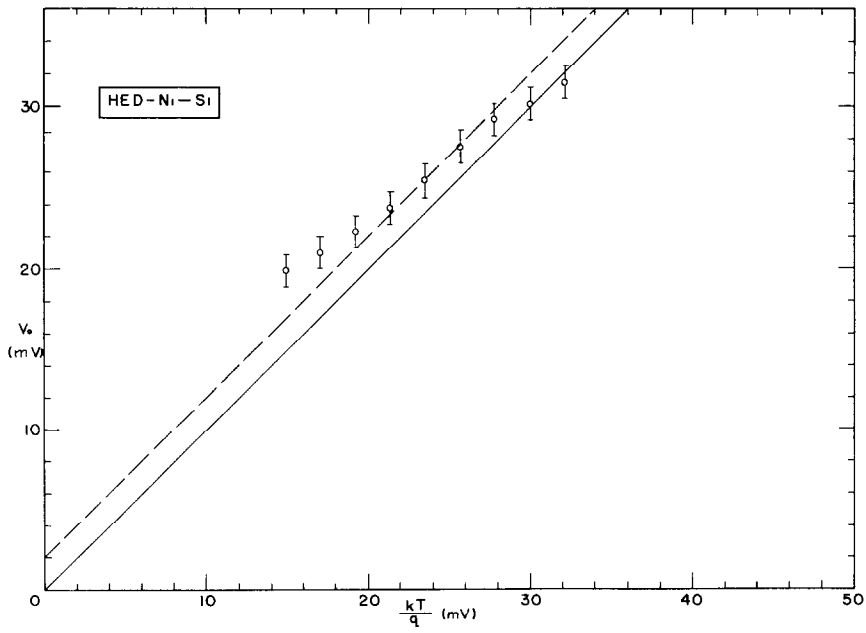

Fig. 6. Plot of V_0 versus kT/q for Ni–Si Schottky barrier diode. Dashed line is drawn parallel to the unity slope (solid) line to illustrate deviation from eqs. (4) and (7).

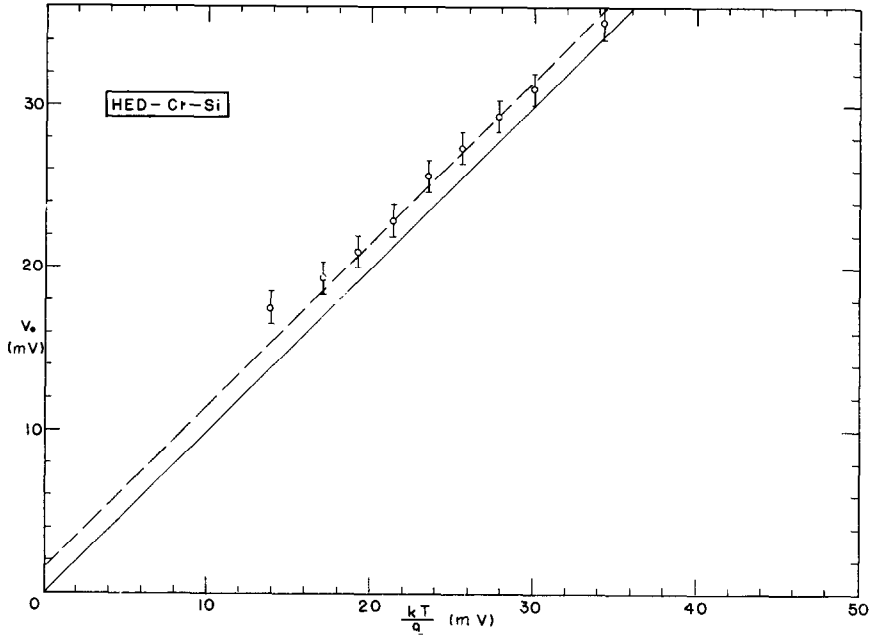

Fig. 7. Plot of V_0 versus kT/q for Cr–Si Schottky barrier diode. Dashed line is drawn parallel to the unity slope (solid) line to illustrate deviation from eqs. (4) and (7).

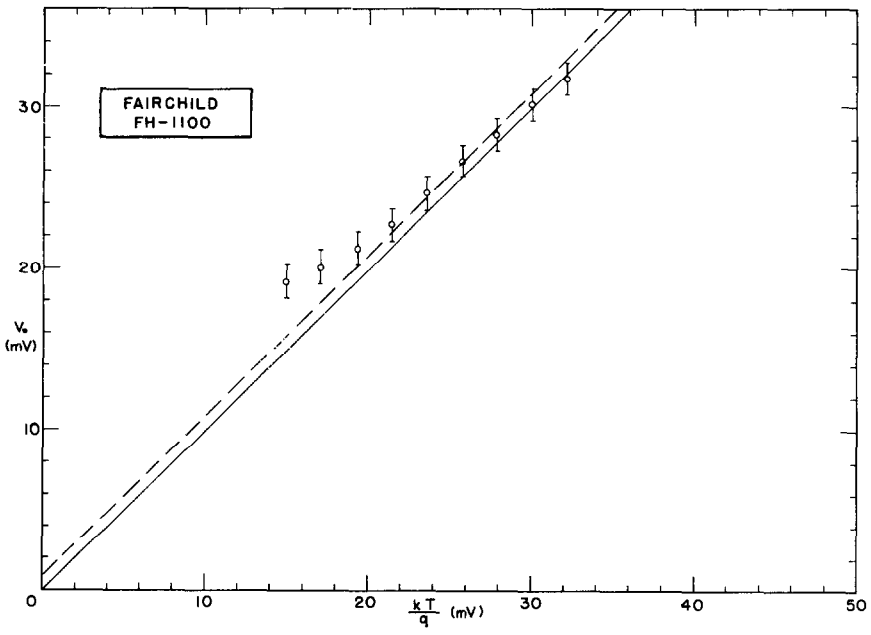

Fig. 8. Plot of V_0 versus kT/q for Fairchild's FH-1100 Schottky barrier diode. Dashed line is drawn parallel to the unity slope (solid) line to illustrate deviation from eqs. (4) and (7).

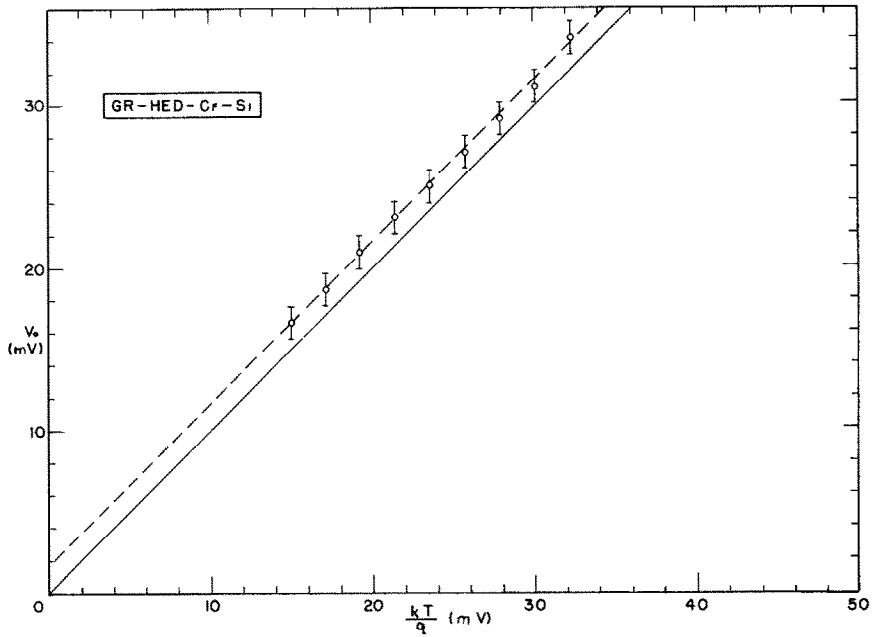

Fig. 9. Plot of V_0 versus kT/q for Cr–Si Schottky barrier diode with a Au–Si guard ring. Dashed line drawn parallel to the unity slope (solid) line fits the data nicely. This means that eq. (7) holds for the I–V behavior of Schottky barrier diodes in which the fringing high electric fields have been eliminated.

slope line labelled as 3 in fig. 2. The same behavior is observed for HP-2900 in fig. 10. This diode has a guard ring and a mesa structure which eliminate the high electric fields from the edge of the diode. No deviation at low temperatures, as observed in figs. 5–8 for non-guard ring structures, are found.

Fig. 11 shows the V_0 versus kT/q data for a Cr–Si$^+$ diode fabricated on a degenerate ($N_D > 10^{18}$ cm^{-3}) n-type Si. It is observed that the data may be fitted with a straight line similar to straight line labelled as 5 in fig. 2.

The above data show that if the high electric fields from the edge of the Schottky barrier diodes are eliminated by using a guard ring or a mesa structure, the I–V behavior of the Schottky barrier is described quite well by eq. (7). The excess temperature term T_0 in the exponent of eq. (7) is heretofore unexplained from the theoretical standpoint. We shall see in section 5 that T_0 can be accounted for by introducing the temperature dependence of the work function of the metal ϕ_M. It should be pointed out that a better fit to the V_0 versus kT/q data plotted in figs. 5–10 is obtained with a straight line similar to that labelled as 3 rather than that labelled as 2 in fig. 2. This shows that eq. (7) describes the I–V behavior of the Schottky barrier diodes better

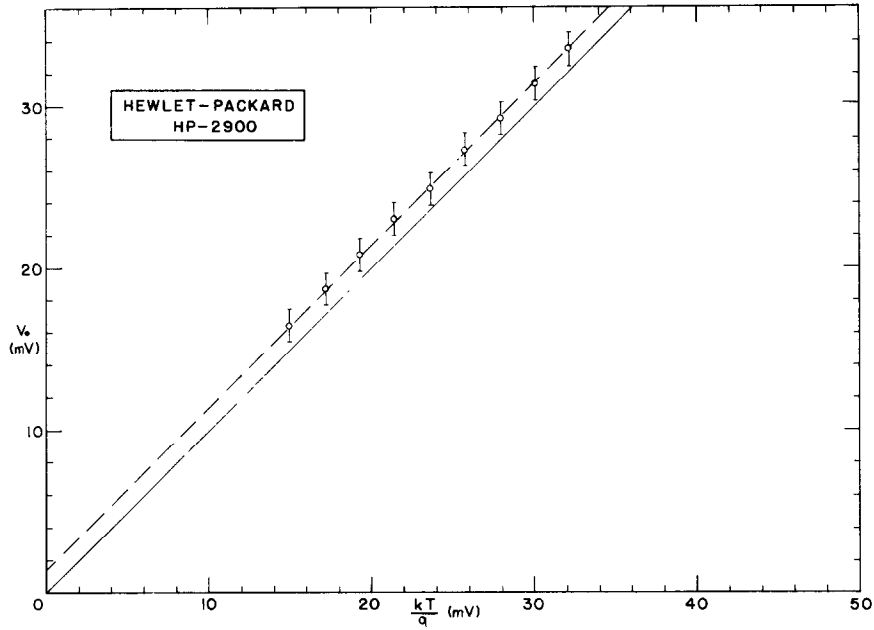

Fig. 10. Plot of V_0 versus kT/q for Hewlett–Packard's HP-2900 which has a Ni–Si Schottky barrier surrounded by Au–Si which acts as a guard ring. Dashed line drawn parallel to the unity slope (solid) line fits the data nicely. This means that eq. (7) holds for the I–V behavior of Schottky barrier diodes in which the fringing high electric fields have been eliminated.

than eq. (6). At a given temperature T, eq. (7) may be expressed in the form of eq. (6) by using eq. (8). However, to check whether eq. (7) or eq. (6) describes the I–V behavior of Schottky barrier diodes, it is necessary to analyze the I–V data as a function of temperature as discussed above.

4. Calculation of ϕ_{MS}

I_s is determined at different temperatures for various diodes from $\ln I$ versus V plots as discussed in section 1. If the ideal Schottky theory would hold, then I_s/T^2 versus $1/T$ will be a straight line whose slope, i.e., change in $1/T$, $\Delta(1/T)$, for a decade change in I_s/T^2 is related to ϕ_{MS} as,

$$\phi_{MS} = \frac{0.1985}{\Delta(1/T)}\ \text{eV}. \tag{18}$$

However, if the ideal Schottky theory does not hold, and if an equation of the type eq. (7) containing an excess temperature in the exponent holds (as found in the discussion above), then I_s/T^2 versus $1/(T+T_0)$ will be a straight line. The latter is found to be true as shown in figs. 12–17 for Au–Si, Ni–Si,

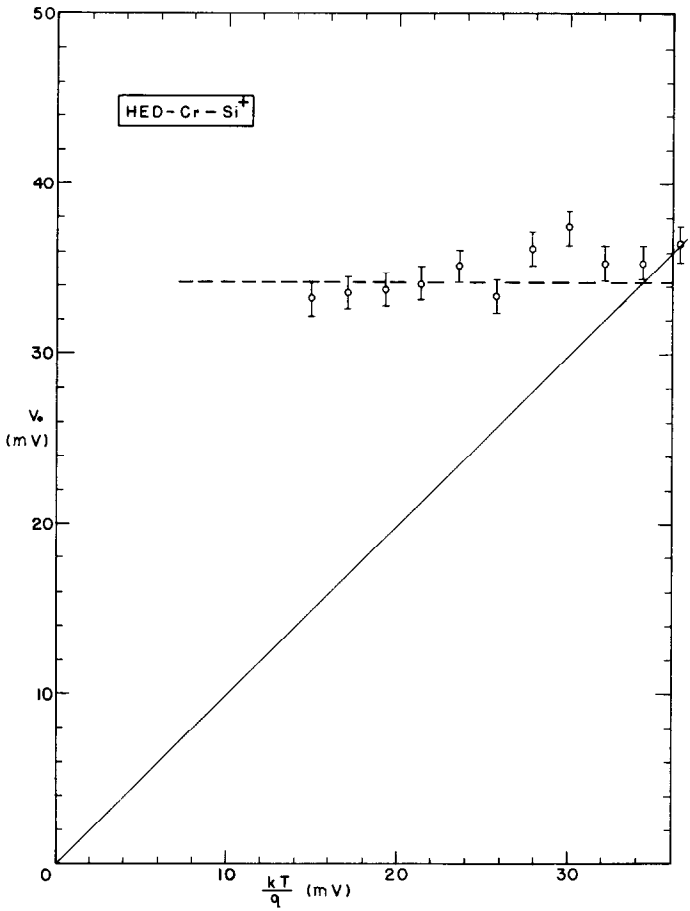

Fig. 11. Plot of V_0 versus kT/q for Cr–degenerate Si ($N_D > 2 \times 10^{18}$ cm^{-3}) Schottky barrier diode. It is observed that V_0 is more or less a constant with temperature implying that tunnelling is dominant in Schottky barriers on degenerate Si.

Cr–Si, FH-1100, Cr–Si-guard ring and HP-2900 diodes, respectively. The data are also plotted versus $1/T$ and it is clear that they cannot be fitted with a straight line. In plotting the data in figs. 12–15, T_0 was not considered to be a constant, because the fringing fields were present in these diodes which cause some thermionic emission to occur. Rather, T_0 was evaluated at different temperatures from the equation,

$$T_0 = (qV_0/k) - T. \tag{19}$$

The fact that the I_s/T^2 versus $1/(T+T_0)$ data can be fitted nicely with a straight line for guard ring and for non-guard ring structures (for which the V_0 data deviates from the straight line at low temperature) in figs. 12–17,

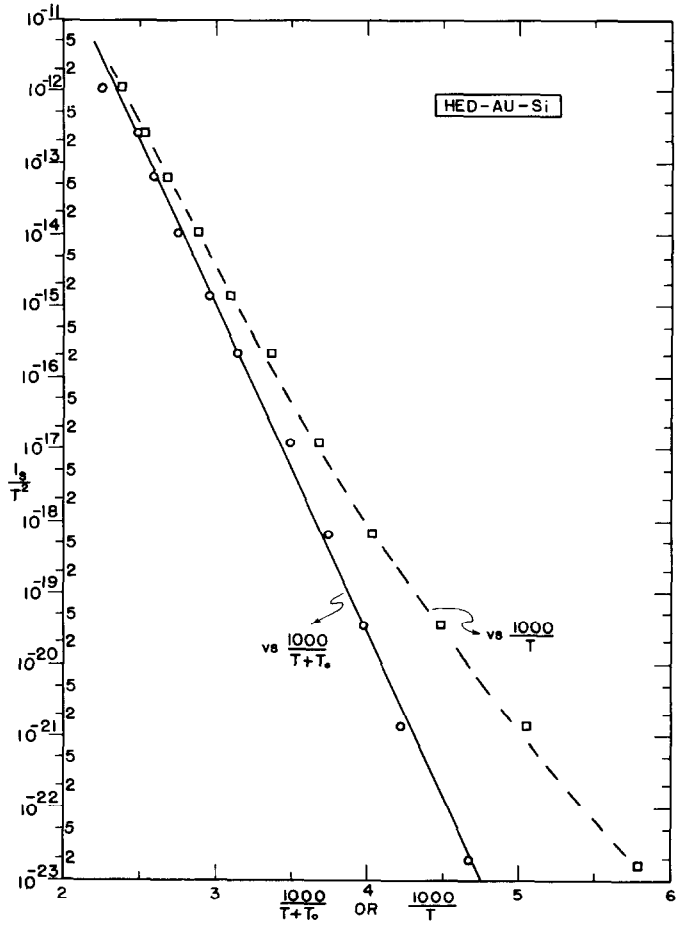

Fig. 12. Plot of I_s/T^2 versus $1000/(T+T_0)$ (solid line) and versus $1000/T$ (dashed line) for Au–Si Schottky barrier diode. The data plotted versus $1000/(T+T_0)$ fit a straight line, whereas those plotted versus $1000/T$ do not fit a straight line.

shows that the saturation characteristics of all the diodes are described well by,

$$I_s = A^* T^2 \, e^{-\phi_{MS0}/k(T+T_0)}. \tag{20}$$

The area of the diode and the effective mass of the electrons do not enter in the above calculation. ϕ_{MS0} is the effective barrier height independent of temperature. As is clear from figs. 9 and 10, T_0 is a constant when the high electric fields are eliminated from the edge of the diode; however, T_0 depends on temperature when the high electric fields are not eliminated from the edge of the diode. For either case, eq. (7) describes well the I–V behavior of the Schottky diodes when eq. (20) is used for I_s.

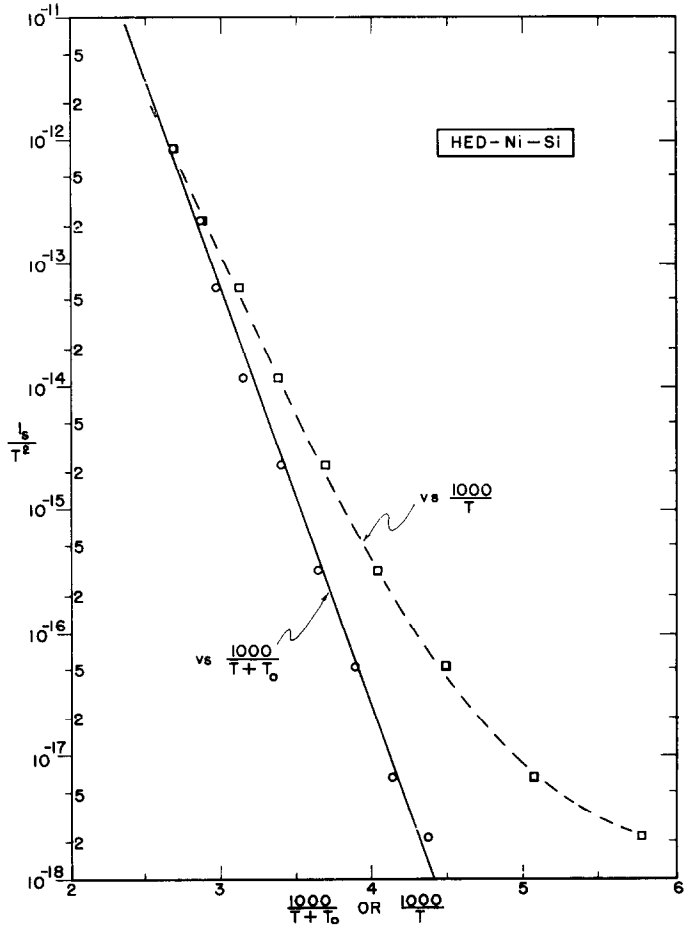

Fig. 13. Plot of I_s/T^2 versus $1000/(T+T_0)$ (solid line) and versus $1000/T$ (dashed line) for Ni–Si Schottky barrier diode. The data plotted versus $1000/(T+T_0)$ fit a straight line, whereas those plotted versus $1000/T$ do not fit a straight line.

Table 1 gives the values of the effective barrier heights ϕ_{MS0} calculated from figs. 12–17, barrier heights ϕ_{MS} at 298 °K for various diodes (see section 5), and T_0 for the guard ring diodes of Cr–Si and HPA-2900 (Ni–Si).

5. Discussion

The concept of temperature independent barrier height ϕ_{MS0} introduced in the present analysis of the I–V data of the Schottky barrier diodes is a new one. It shows up naturally from the plots of $\ln(I_s/T^2)$ versus $1/(T+T_0)$ in figs. 12–17 which are straight lines as predicted by eq. (20). It is interesting

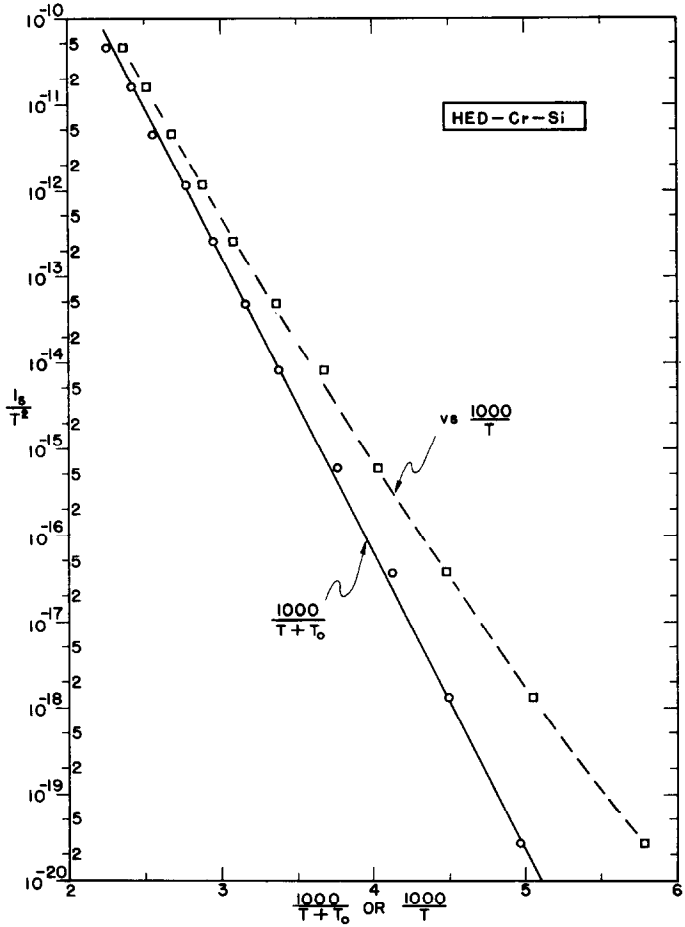

Fig. 14. Plot of I_s/T^2 versus $1000/(T+T_0)$ (solid line) and versus $1000/T$ (dashed line) for Cr–Si Schottky barrier diode. The data plotted versus $1000/(T+T_0)$ fit a straight line, whereas those plotted versus $1000/T$ do not fit a straight line.

TABLE 1

Metal–Si system	ϕ_{MS0} (eV)	ϕ_{MS} at $T=298$ °K (eV)	T_0 (°K)
Au–Si	0.90	0.81	
Ni–Si	0.68	0.64	
Cr–Si	0.68	0.62	
Cr–Si (guard ring)	0.68	0.61	34
Fairchild FH-1100	0.70	0.64	
HPA-2900 (Ni–Si)	0.68	0.63	24

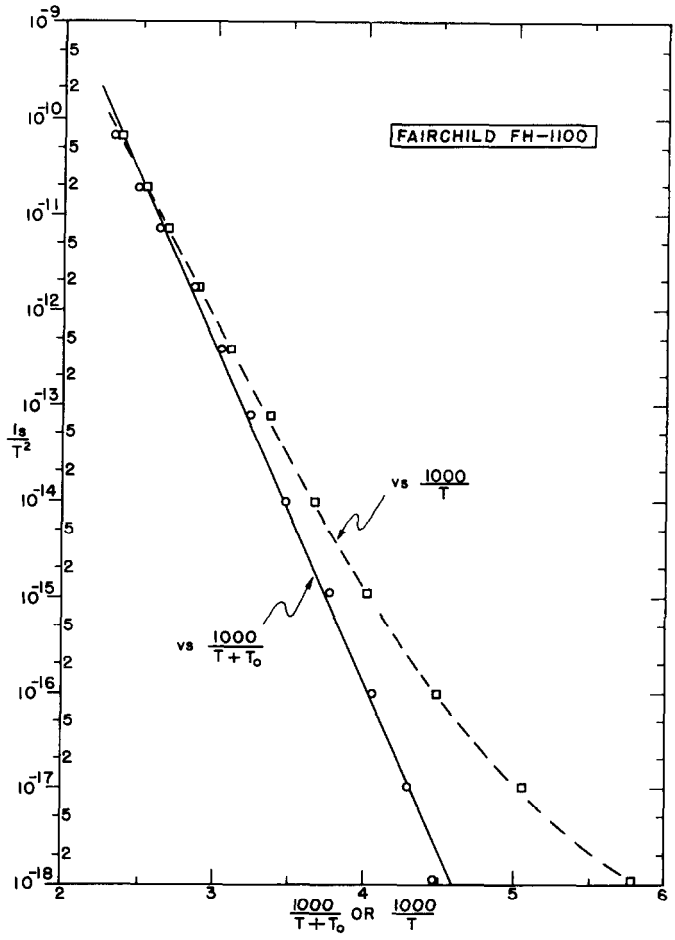

Fig. 15. Plot of I_s/T^2 versus $1000/(T+T_0)$ (solid line) and versus $1000/T$ (dashed line) for Fairchild's FH-1100 Schottky barrier diode. The data plotted versus $1000/(T+T_0)$ fit a straight line, whereas those plotted versus $1000/T$ do not fit a straight line.

to note that these linear plots characteristic of ϕ_{MS0} are obtained both for guard ring as well as non-guard ring structures. T_0 was evaluated at each temperature using eq. (19). It was more or less a constant with respect to temperature for the guard ring diodes and it increased at lower temperatures for non-guard ring diodes. Although a detailed calculation has not been attempted here, a qualitative understanding of ϕ_{MS0} and T_0 can be obtained by the following first order calculation.

The surface preparation of Si to fabricate Schottky barrier diodes involves chemical etching of the oxide layer from Si and evaporation of a metal in a

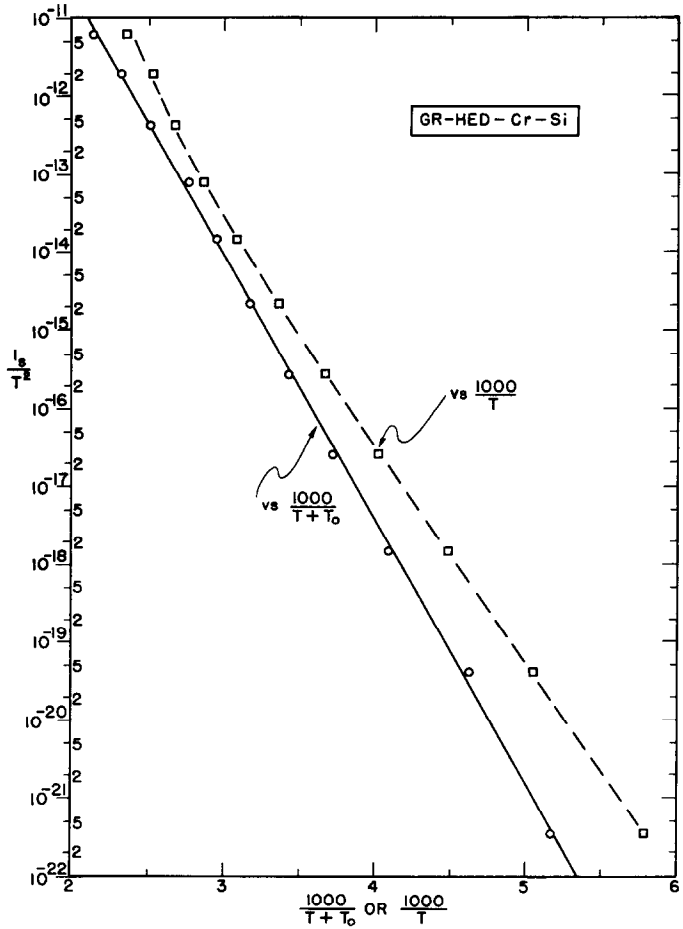

Fig. 16. Plot of I_s/T^2 versus $1000/(T+T_0)$ (solid line) and versus $1000/T$ (dashed line) for Cr–Si Schottky barrier diode with a Au–Si guard ring. The data plotted versus $1000/(T+T_0)$ fit a straight line, whereas those plotted versus $1000/T$ do not fit a straight line.

vacuum system. Such fabrication techniques make the surface state density in Si lower than that obtained by cleaving Si in an evaporating stream of the metal. Therefore, in the present discussion, it is assumed that the barrier height ϕ_{MS} is governed more or less by the work function difference model, i.e., eq. (3). (For atomically clean surfaces, as in the cleaved case, the surface state model, eq. (1) is dominant – see discussion in section 1.) Further, it is assumed that the electron affinity, χ, of Si is temperature independent[11]). Therefore, the temperature dependence of ϕ_{MS} will follow that of ϕ_M (see fig. 3).

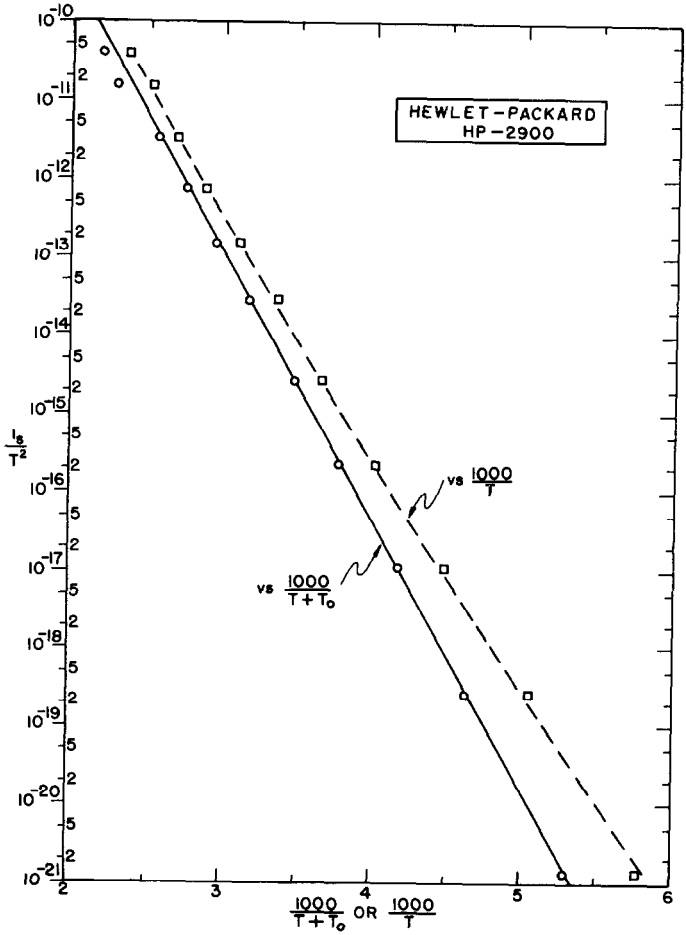

Fig. 17. Plot of I_s/T^2 versus $1000/(T+T_0)$ (solid line) and versus $1000/T$ (dashed line) for Hewlett-Packard's HP-2900 Schottky barrier diode. The data plotted versus $1000/(T+T_0)$ fit a straight line, whereas those plotted versus $1000/T$ do not fit a straight line.

Let the temperature dependence of ϕ_M be given by,

$$\phi_M = \phi_0 - \alpha T - \beta T^2 - \gamma T^3 - \cdots \simeq \phi_0 - \alpha T. \tag{21}$$

where the higher order terms have been neglected. ϕ_0 is the temperature independent part of the work function. Therefore, the temperature dependence of ϕ_{MS} can be written as,

$$\phi_{MS} \simeq \phi_{MS0} - \alpha T, \tag{22}$$

where ϕ_{MS0} is the temperature independent part of the barrier height defined

by,

$$\phi_{MS0} = \phi_0 - \chi . \tag{23}$$

The fact that I_s/T^2 versus $1/T$ plots in figs. 12–17 are not linear suggests that ϕ_{MS} is neither a constant with respect to temperature nor does it have a linear temperature dependence. Nevertheless, the first order calculation using eq. (22) is given below to illustrate that a term like T_0 in eq. (7) can arise from the temperature dependence of ϕ_{MS}.

The saturation current I_s at a given temperature T according to Schottky theory is given by eq. (5), rewritten here for convenience,

$$I_s = A^* T^2 \, e^{-\phi_{MS}/kT} . \tag{5}$$

The experimental data of $\ln (I_s/T^2)$ versus $1/T$ do not, however, yield a straight line as discussed in section 4. This suggests that ϕ_{MS} is not a constant with respect to the temperature. Let us introduce the temperature dependence of ϕ_{MS} as defined by eq. (22) in eq. (5). Therefore,

$$I_s = A^* T^2 \, e^{-(\phi_{MS0} - \alpha T)/kT} . \tag{24}$$

In eq. (24), we have used simple Schottky theory [1]) except that the barrier height is no longer assumed to be invariant of temperature. Now the experimental data of figs. 12–17 show that they obey eq. (20) because $\ln (I_s/T^2)$ versus $1/(T+T_0)$ is linear. This shows that the effective barrier height in eq. (20) is temperature independent, and it is the same as ϕ_{MS0} defined by eq. (23). Therefore, comparing the empirical equation, eq. (20), with the theoretical equation, eq. (24), we get,

$$(\phi_{MS0} - \alpha T)/kT = \phi_{MS0}/k(T + T_0)$$

or

$$\alpha = \phi_{MS0}/T(1 + T/T_0) . \tag{25}$$

Eq. (25) shows that in this first order formalism, α is not a constant, independent of temperature. For more accurate calculation, higher order terms in eq. (21) should be retained. Table 2 lists the average values of α for the entire temperature range (173–423 °K) for the various diodes studied. Also listed are the temperature coefficients of ϕ_M determined by other techniques. That the work function difference model assumed above to describe the barrier height formation and its temperature dependence is a better assumption for the diodes studied than the surface state model, is evidenced by the fact that ϕ_{MS0} for Au is quite different than that for Cr–Si and Ni–Si. The fact that ϕ_{MS0} for the latter two are similar is coincidental in that the ϕ_M's are similar. If the surface state model were to apply, all ϕ_{MS} values irrespective of the metal used would have been equal.

TABLE 2

Element	This work		Other work			
	Avg. α (eV/°K)	Temp. range (°K)	α (eV/°K)	Temp. range (°K)	Method used	Ref.
Au	30×10^{-5}	173–423				
Ni	14×10^{-5}	173–423	$< \pm 1.6 \times 10^{-5}$	1170–1250	Thermionic emission	13
Cr	18.2×10^{-5}	173–423	$< \pm 3.2 \times 10^{-5}$	1100–1400	Thermionic emission	13
Cr (guard-ring structure)	23.6×10^{-5}	173–423				
Cr(?) (Fairchild FH-1100)	21×10^{-5}	173–423				
Ni (HPA-2900)	16.1×10^{-5}	173–423	$< \pm 1.6 \times 10^{-5}$	1170–1250	Thermionic emission	13

The above calculations suggest that the excess temparature T_0 can be accounted for by using the temperature dependent barrier height in the simple Schottky equation.

The data presented in figs. 5–10 can be explained by the thermionic field emission calculations of Crowell and Rideout[12]). A more detailed comparison with their theory will be presented elsewhere.

Acknowledgment

The author would like to thank C. R. Crowell (University of Southern California), F. M. Fowkes, J. C. McDade and F. A. Padovani (Texas Instruments) for helpful discussions. Thanks are also due D. Varady for data taking and performing the analysis to determine V_0 accurately at high temperatures, and to C. R. Crowell and T. Fischer (Yale University) for sending preprints of their work.

References

1) W. Schottky, Physik. Z. **32** (1931) 833.
2) J. Bardeen, Phys. Rev. **71** (1947) 717
3) C. A. Mead and W. Spitzer, J. Appl. Phys. **34** (1963) 3061; Phys. Rev. Letters **10** (1963) 471;
C. A. Mead, Solid-State Electron. **9** (1966) 1023.
4) C. R. Crowell, S. M. Sze and W. G. Spitzer, Appl. Phys. Letters **4** (1964) 91.
5) H. K. Henisch, *Rectifying Semiconductor Contacts* (Oxford at the Clarendon Press, 1957) p. 182.
6) M. M. Atalla, R. W. Soshea, R. C. Lucas, D. A. Reid and V. M. Dowler, Investigation of Hot Electron Emitter, Scientific Report No. 3, AFCRL-63-113, February 1963.
7) S. M. Sze, C. R. Crowell and D. Kahng, J. Appl. Phys. **35** (1964) 2534.
8) F. A. Padovani and G. G. Sumner, J. Appl. Phys. **36** (1965) 3744.
9) A. N. Saxena and D. Varady, to be published.
10) F. A. Padovani and R. Stratton, Solid-State Electron. **9** (1966) 695.
11) T. Fischer, private communication.
12) C. R. Crowell and V. L. Rideout, to be published and private communication.
13) R. G. Wilson, J. Appl. Phys. **37** (1966) 2261.